

1 **Patterns of speciation are similar across mountainous and lowland regions for**
2 **a Neotropical plant radiation (Costaceae: *Costus*)**

3 Running Title: Speciation in Neotropical *Costus*

4
5 Oscar M. Vargas^{1,2,3}, Brittany Goldston⁴, Dena L. Grossenbacher⁴, Kathleen M. Kay¹

6
7 ¹Department of Ecology and Evolutionary Biology, University of California, Santa Cruz, Santa
8 Cruz, California 95060

9 ²Department of Biological Sciences, Humboldt State University, Arcata, California 95521

10 ³Email: oscarvargash@gmail.com

11 ⁴Department of Biology, California Polytechnic State University, San Luis Obispo, California
12 93401

13
14 **Author Contributions:** Study was designed by OMV, DLG and KMK. KMK curated the plant
15 collection used for genomic sampling. OMV, DLG and KMK collected the data. Phylogenetic
16 analyses were conducted by OMV. Species richness and topographic complexity analyses were
17 conducted by BG; all other geographic and climatic analyses were conducted by DLG.

18 Manuscript was written jointly by OMV, DLG, and KMK.

19
20 **Acknowledgments:** This research was funded by NSF Dimensions of Biodiversity grant DEB-
21 1737878 to KMK, DLG, Jennifer Funk (Chapman University), Santiago Ramirez (UC Davis),
22 and Carlos Garcia-Robledo (U Conn). We thank the Organization for Tropical Studies,
23 Tortuguero National Park, Estación Biológica Monteverde, and Estación Tropical La Gamba for

24 facilitating field work in Costa Rica. We also thank the Smithsonian Tropical Research Institute
25 for facilitating field work in Panama. We thank Julia Harenčár, Rossana Maguiña, Eleinis Ávila-
26 Lovera, and Pedro Juarez for help with field collecting, and Edgardo Ortiz for assistance with the
27 analysis of the transcriptomic data. All field research was conducted with appropriate collection
28 permits in Costa Rica (M-P-SINAC-PNI-ACAT-026-2018, ACC-PI-027-2018, M-PC-SINAC-
29 PNI-ACLAP-020-2018, INV-ACOSA-076-18, M-PC-SINAC-PNI-ACTo-020-18, and
30 CONAGEBIO R-056-2019-OT and R-058-2019-OT), Panama (SE/AP-13-19), and Peru
31 (Resolución Jefatural N° 007-2017-SERNANP-RNAM-JEF and Resolución de Dirección
32 General N° 231-2017-SERFOR/DGGSPFFS both granted by Servicio Nacional Forestal y de
33 Fauna Silvestre del Estado Peruano). Additional plant samples were graciously contributed by
34 John Kress, Douglas Schemske, Dave Skinner, the National Tropical Botanical Garden, and the
35 MICH, MO, UC, and US herbaria. We thank Jim Velzy, Sylvie Childress, and Sarah Ashlock for
36 greenhouse care of the living *Costus* collection, Hannah Thacker and Jaycee Favela for help with
37 lab work, and Russell White and Andrew Fricker for help with the topographic complexity
38 analysis.

39 **Data Accessibility Statement:** Raw sequence data can be found in GenBank (Tables S1-
40 S2). Data, control files, and custom scripts can be accessed in Dryad
41 <https://doi.org/10.5061/dryad.p8cz8w9nk>, custom code can also be found at
42 https://bitbucket.org/oscarvargash/costus_speciation

43

44

45

46 **Patterns of speciation are similar across mountainous and lowland regions for**
47 **a Neotropical plant radiation (Costaceae: *Costus*)**

48 *Abstract*

49 High species richness and endemism in tropical mountains are recognized as major contributors
50 to the latitudinal diversity gradient. The processes underlying mountain speciation, however, are
51 largely untested. The prevalence of steep ecogeographic gradients and the geographic isolation
52 of populations by topographic features are predicted to promote speciation in mountains. We
53 evaluate these processes in a species-rich Neotropical genus of understory herbs that range from
54 the lowlands to montane forests and have higher species richness in topographically complex
55 regions. We ask whether climatic niche divergence, geographic isolation, and pollination shifts
56 differ between mountain-influenced and lowland Amazonian sister pairs inferred from a 756-
57 gene phylogeny. Neotropical *Costus* ancestors diverged in Central America during a period of
58 mountain formation in the last 3 My with later colonization of Amazonia. Although climatic
59 divergence, geographic isolation, and pollination shifts are prevalent in general, these factors
60 don't differ between mountain-influenced and Amazonian sister pairs. Despite higher climatic
61 niche and species diversity in the mountains, speciation modes in *Costus* appear similar across
62 regions. Thus, greater species richness in tropical mountains may reflect differences in
63 colonization history, diversification rates, or the prevalence of rapidly evolving plant life forms,
64 rather than differences in speciation mode.

65

66 Keywords: Ecological specialization, diversification, geographic isolation, Neotropics,
67 pollination shifts, spiral gingers.

68 *Introduction*

69 Tropical mountains exhibit extreme species richness and endemism, contribute
70 substantially to latitudinal diversity gradients, and are thought to be cradles of recent speciation
71 (Rahbek et al. 2019a, Rahbek et al. 2019b). The Neotropics contain some of the world's most
72 species-rich plant diversity hotspots (Barthlott 2005), which all contain substantial mountain
73 ranges. Mountains are hypothesized to play two major roles in the process of speciation: the
74 generation of steep environmental gradients over geographic space (ecogeographic gradients)
75 sensu Gentry (1982) and the geographic isolation of populations by topographic features sensu
76 Janzen (1967). Although studies have linked the timing of montane diversifications with
77 mountain building (Luebert and Wigend 2014), mechanisms by which tropical mountains may
78 promote speciation remain unclear, in part because well-resolved species-level phylogenies for
79 tropical clades remain rare.

80 Steep montane gradients, in factors such as climate or biotic communities, could promote
81 speciation by ecogeographic divergence without sustained allopatry (Gentry 1982; Angert and
82 Schemske 2005; Hughes and Atchison 2015; Pyron et al. 2015). For example, a marginal
83 population may adapt to novel climate conditions at a species' upper or lower elevation range
84 limit, at the cost of adaptation to climatic conditions in the remainder of the species' range
85 (Angert et al. 2008). Similarly, biotic communities (Dobzhansky 1950), such as pollinator
86 assemblages, turnover rapidly in Neotropical mountains (Stiles 1981) and likely contribute to
87 pollinator isolation in plants (Gentry 1982; Kay et al. 2005; Lagomarsino et al. 2016). Taken
88 together, mountains provide large climatic and biotic niche space across short geographic
89 distances, providing an arena for divergent selection and speciation.

90 Topographic features also can drive allopatric speciation by serving as dispersal barriers
91 regardless of ecogeographic divergence. For example, a species' range may be divided by a
92 newly formed topographic barrier or individuals may disperse across ridges or valleys to distant
93 areas of suitable habitat. If tropical organisms have narrower climatic tolerances than temperate
94 ones, as hypothesized, the effect of topographic features on isolation may be greatly magnified in
95 tropical mountains (Janzen 1967; Ghalambor et al. 2006; Cadena et al. 2012; Guarnizo and
96 Canatella 2013). Topographic dispersal barriers may lead to frequent progenitor-derivative, or
97 budding speciation, in mountain-influenced areas. This mode of speciation (hereafter, budding)
98 occurs when an initially small colonizing population becomes reproductively isolated from a
99 larger-ranged species (Mayr 1954), and is in contrast to vicariant speciation where a geographic
100 barrier bisects a species' range (Mayr 1982). Whereas budding speciation may be common in
101 mountains, it is likely less common in lowlands due to fewer steep climatic gradients and
102 topographic barriers.

103 These long-standing hypotheses about dispersal barriers and ecogeographic gradients in
104 tropical mountains predict unique signatures of speciation. Moreover, if mountains *per se* are
105 driving speciation, patterns of speciation in mountains should differ from lowland regions, which
106 have shallow climatic gradients and less turnover in biotic communities relative to mountains
107 (De Cáceres et al. 2012; Pomara et al. 2012; Fig. 1). First, if ecogeographic divergence is of
108 primary importance, sister species occurring in or around mountains (hereafter, mountain-
109 influenced) are predicted to show climatic niche differentiation (Fig. 1E), and this differentiation
110 should be greater on average than in lowland species pairs (Fig. 1A-B). Similarly, pollinator
111 shifts are predicted to be more frequent in mountain-influenced sister pairs than in the lowlands
112 because of ecogeographic gradients in pollinator assemblages. Second, if topographic dispersal

113 barriers are of primary importance, mountain-influenced sister pairs should frequently show
114 geographic isolation (Fig. 1D), and this isolation should be greater than in lowland species pairs
115 (Fig. 1A), for which geographic isolation may be more ephemeral. If topographic dispersal
116 barriers promote budding speciation, we further predict: 1) greater range size asymmetry
117 between mountain-influenced relative to lowland sister pairs, especially in younger pairs
118 (Barracough and Vogler 2000; Fitzpatrick and Turelli 2006; Grossenbacher et al. 2014), and 2)
119 nested phylogenetic relationships between recently-diverged mountainous sister species,
120 indicating that small-ranged taxa are derived from widespread progenitors (e.g., Baldwin 2005).

121 Ecogeographic gradients and topographic dispersal barriers in mountains also predict
122 different patterns of range overlap with divergence time. If allopatric speciation is dominant,
123 then more recently-diverged species pairs should be completely allopatric, whereas older pairs
124 might show range overlap due to range shifts since speciation (Fitzpatrick and Turelli 2006).
125 Contrastingly, if parapatric speciation across ecogeographic gradients is dominant, younger sister
126 species pairs should show partial range overlap whereas older pairs should show a variety of
127 configurations (Fitzpatrick and Turelli 2006; Anacker and Strauss 2014). It is also possible that
128 geographic isolation and niche divergence commonly work together to promote speciation in
129 mountains, with geographically isolated populations adapting to new climate niches (Fig. 1F).

130 Here we examine speciation modes in the Neotropical spiral gingers (*Costus* L.), a genus
131 comprising approximately 59 species found from sea level to cloud forests throughout tropical
132 Central and South America. *Costus* is a pantropical genus of perennial monocot herbs with a
133 species-rich Neotropical clade nested within the relatively species-poor African taxa. The
134 Neotropical clade likely arose via long-distance dispersal from Africa (Kay et al. 2005, Salzman
135 et al. 2015). Neotropical *Costus* are widely interfertile (Kay and Schemske 2008) with stable

136 ploidy (Maas 1972; 1977). Prior studies have suggested a prominent role for prezygotic
137 reproductive barriers, including ecogeographic isolation (Chen and Schemske 2015), differences
138 in pollination syndrome (orchid bee v. hummingbird; Kay and Schemske 2003), and floral
139 divergence within a pollination syndrome (Kay 2006; Chen 2013). We begin by documenting
140 that *Costus* species richness is indeed higher in Neotropical areas with high topographical
141 complexity, consistent with mountains being strong drivers of speciation in *Costus* (assuming
142 similar extinction rates). We then infer a multi-locus phylogeny for *Costus* that we use to
143 reconstruct the biogeographic history, the timing of divergence, and the evolution of pollination
144 syndromes in the genus. Finally, we use sister species comparisons to test our predictions about
145 speciation modes in montane regions using climatic, geographic, and pollination data. We
146 discuss how our results shed light on speciation in the Neotropics.

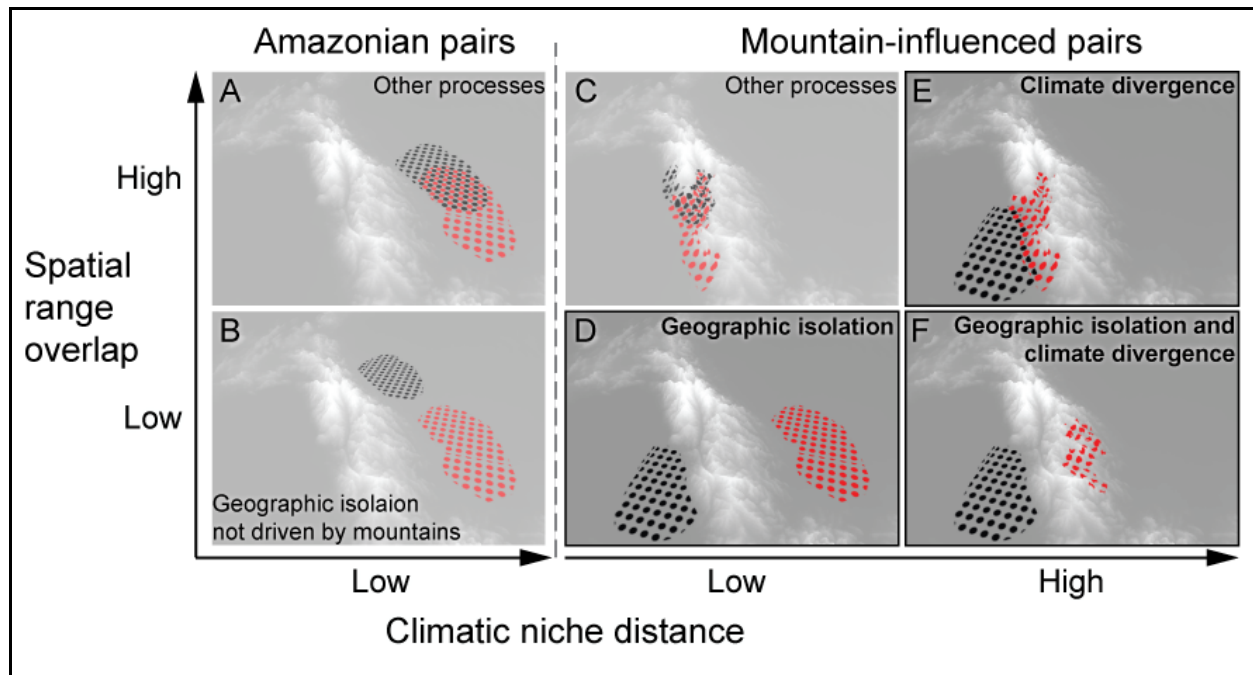


FIGURE 1. Testing the role of mountains in speciation. Hypothetical ranges of sister species, as black and red filled circles, overlaid on a landscape where lighter grays indicate higher elevations. Sister species in Amazonia, a region with low topographic complexity and relatively homogeneous climate, are expected to be partially sympatric (A) or geographically isolated (B) by lowland geological features, fine-scale habitat divergence, or biotic interactions. Mountain-influenced sister species may also show these patterns (C), however, we predict that geographic isolation (D), climate niche divergence (E), or both (F) will be more common in mountains than in the lowlands (indicated by bolded boxes).

147 *Material and Methods*

148 **OCCURRENCE DATA**

149 We downloaded all known occurrence records for the species in our study from the
150 Global Biodiversity Information Facility (GBIF, <http://www.gbif.org>). We supplemented these
151 with occurrences from our own field studies in 2018 and 2019, as well as additional herbarium
152 (Cornell, MSU, and UC JEPS) and iNaturalist data (<https://www.inaturalist.org>). All occurrences
153 were then filtered for quality by excluding records without decimal accuracy in latitude and
154 longitude, and with coordinates failing to match the locality description. To avoid potential
155 taxonomic misidentifications, we retained only occurrences where the identification was made
156 by one of three taxonomic experts: Paul Maas, Dave Skinner, or KMK. We checked species'
157 epithets against the most recently published taxonomies and corrected synonyms and spelling
158 errors. The final filtered dataset included 4,834 unique occurrences for 61 taxa (mean per
159 taxa=79, range=1-593, SD=121).

160 **TOPOGRAPHIC COMPLEXITY AND SPECIES RICHNESS**

161 To quantify topographic complexity across our study region, we used the terrain
162 ruggedness index (TRI) function in ArcGIS (ESRI 2018). TRI is a measure of topographic
163 heterogeneity that takes the sum in elevation change between a focal grid cell and all
164 neighboring grid cells (Riley et al. 1999). To calculate TRI, we used raw elevation data at 1km
165 resolution from earthenv.org/topography and projected it to 1600 and 6400 km² grids. The two

166 grid sizes allowed us to assess whether our results were sensitive to spatial scale. Species
167 richness per grid cell was recorded as the number of unique species occurrences in the filtered
168 occurrence data described above (Point Statistics function in ArcGIS). Richness, TRI values, and
169 X,Y coordinates for each grid cell were extracted across the two spatial scales and saved for
170 downstream analysis (Extract Multi Values to Point function in ArcGIS).

171 To determine whether species richness is predicted by the terrain ruggedness index (TRI),
172 we used both an ordinary least squares regression model and a spatial autoregressive lag model.
173 Ecological data is typically affected by spatial autocorrelation (SAC), with nearby localities
174 being more similar than expected when random (Kissling and Carl 2008). As a result of species
175 distributions being spatially constructed by nature, our data will likely have residual SAC,
176 breaking an assumption of linear regression. To check for residual SAC between TRI and species
177 richness we used Moran's I coefficient. A Moran's I coefficient near zero indicates no SAC,
178 while positive and negative values indicate positive or negative autocorrelation (Bhattarai et al.
179 2004). Spatial autoregressive models are commonly used to mitigate known SAC in the
180 residuals. Accordingly, we used a spatial autoregressive lag model to relate species richness and
181 TRI. Due to the ongoing debate of incorporating spatial autocorrelation into the analysis of
182 species distribution data, we chose to compare our model results to an ordinary least squares
183 regression model which ignores spatial autocorrelation (Dormann 2007). Model selection was
184 accomplished using the Akaike information criterion (AIC).

185 Because comparisons of species richness may be impacted by uneven sampling across
186 regions (Gotelli and Colwell, 2001), we performed a rarefaction analysis to ensure that our
187 results were not driven by greater sampling effort in mountains relative to lowlands. To do this,
188 we classified all occurrences as either mountainous ($TRI > 5$, $N=3477$) or lowland ($TRI \leq 5$,

189 N=1140). We then randomly drew an equal number of occurrences from the two samples
190 (N=1000), determined richness, and repeated this 1000 times (for a similar approach, see Grytnes
191 and Beaman 2006). Richness in the rarefied samples was considered to significantly differ
192 between mountainous and lowland regions if the 95% confidence intervals were non-
193 overlapping.

194 **PHYLOGENETIC ANALYSIS**

195 To infer a well resolved phylogeny we employed targeted sequencing, capturing 853
196 genes in 113 samples representing 57 species, including outgroups (Table S1) and, when
197 possible, samples from different geographic locations for widespread species and putative
198 progenitor-derivative species pairs. We selected the genes based on six transcriptomes belonging
199 to neotropical *Costus*, five newly sequenced (Table S2) and one published (GenBank
200 BioSample: SAMN00991785). We extracted total RNA using the RNeasy Plant Mini Kit
201 (Qiagen, San Diego, California) from fresh tissue; Poly-A enriched libraries (with an insert size
202 of 300 bp) were prepared by the DNA Technologies Core at the University of California, Davis,
203 with subsequent paired-end 150 bp HiSeq4000 sequencing (Illumina Inc.). We employed
204 SeqyClean v.1.10.07 (Zhbannikov et al. 2017) to remove low quality reads and read tails using
205 default parameters and a cutoff Phred score of 20. Poly A/T tails were also trimmed. Assembly
206 of transcripts was performed with Trinity v2.8.4 (Grabherr et al. 2011). With the transcriptomic
207 dataset, we employed Captus (<https://github.com/edgardomortiz/captus>) to select the genes for
208 sequencing. Briefly, Captus first used VSearch V.2.10.3 (Edgar 2010) to deduplicate individual
209 transcriptomes (query_cov [overlap] = 0.99, id [similarity] = 0.995) and performed clustering
210 among the transcripts of all samples (query_cov = 0.75, id = 0.75) outputting a fasta file for
211 every cluster. Clusters were subsequently aligned with MAFFT v7.407 (Katoh and Standley

212 2013) using the “--auto” mode. Only genes for which a single copy was found in the alignments
213 were used for subsequent subselection, filtering out possible paralogs. Final gene selection for
214 sequencing in the phylogenetic analysis was based on transcript length (len = 720-2400),
215 transcript presence in a minimum of four species (spp= 4,6), transcript presence in a focal
216 species (*Costus pulverulentus*, foc = 1), percentage of gaps in the alignment not exceeding 50%
217 (gap = 50), an average pairwise percentage identity range of 75–99.6% (pid = 75-99.6), and
218 allowing a maximum of 15% of short introns per gene (< 120 bp) (psr = 0.15). Finally, allowing
219 for a G-C content of 30–70% and a tailing percentage overlap of 66.55, Captus designed 16,767
220 baits of 120bp in length for the 853 genes selected.

221 We extracted DNA from recently collected field and greenhouse samples using
222 NucleoSpin Plant Mini Kit II (Macherey-Nagel, Düren, Germany) according to the
223 manufacturer's protocol, adding 5 μ L proteinase K (20 mg/mL) to the digestion step and
224 increasing the digestion incubation time to an hour. For herbarium specimens we used the
225 MagPure Plant DNA LQ kit (Angen Biotech, Guangdong, China). Library preparation and
226 sequencing for the 853 targeted genes was performed by Rapid Genomics (Gainesville, Florida).
227 We employed HybPiper v1.3.1 (Johnson et al. 2016) to assemble the targeted genes, and MAFFT
228 using the “linsi” exhaustive algorithm to align the matrices containing concatenated exons and
229 introns. Problematic sections in the alignments were trimmed with the “-automated1” option of
230 trimAl v1.4.rev22 (Capella-Gutiérrez et al. 2009). Rogue taxa were removed with the “-
231 reoverlap 0.75 -seqoverlap 75” arguments of trimAl.

232 To filter out tentative paralog genes unidentified by Captus, we excluded genes with
233 extreme variation in branch lengths based on the assumption that ingroup branches should not be
234 extremely long considering the recent diversification of Neotropical *Costus* (Kay et al. 2005). To

235 identify genes with extreme in-group branch length variation, we first inferred trees for each
236 alignment with IQ-Tree v1.6.12 (Nguyen et al. 2015) using a GTR+G model and 1000 ultrafast
237 bootstraps. Then, after removing outgroups with pxtmt (Brown et al. 2017) and outlier sequences
238 with TreeShrink “-q 0.10” (Mai and Mirabab 2018), we calculated the variation in branch lengths
239 using SortaDate (Smith et al. 2018), and then sorted genes accordingly. Visual examination of
240 genes with extreme variation in branch lengths revealed possibly paralogy. Therefore, to be
241 conservative we filtered out genes in the top 10% distribution of branch-length variation,
242 resulting in 756 genes for subsequent phylogenetic analysis. Visual examination of remaining
243 genes after filtering revealed no potential paralog issues.

244 We used concatenated- and coalescent-based approaches for the inference of species
245 trees. Before concatenation, gene alignments were filtered from outlier sequences flagged
246 previously by TreeShrink in our gene trees. A matrix containing sequences for 756 genes was
247 used to infer a concatenated-based species tree, using IQ-Tree with an independent GTR+G
248 model of sequence evolution for each gene partition and 1000 ultrafast bootstraps. We calculated
249 the number of gene trees supporting a given node in the concatenated topology by employing
250 phyparts (Smith et al. 2015), and results were plotted with phypartspiecharts.py (<https://github.com/mossmatters/MJPythonNotebooks>). For the coalescent inference, we inferred a species tree
252 based on the 756 IQ-Tree-inferred topologies with ASTRAL v.5.6.3 (Zhang et al. 2017),
253 collapsing branches with less than 90 ultrafast-bootstrap support and removing from each input
254 tree the taxa flagged as having outlier branch lengths.

255 To determine whether *Costus* diversification coincided with substantial mountain uplift,
256 and to estimate divergence time for sister species, we calibrated our concatenated topology using
257 fossils and external non-*Costus* Zingiberales sequences (Table S3). The inclusion of non-*Costus*

258 sequences was necessary because of the absence of *Costus* fossils. First, we identified the top 50
259 most clock-like genes in our dataset using the metrics outputted by SortaDate, considering in
260 order of priority branch-length variance (low variance preferred), root-to-tip length (high length
261 preferred), and topological similarity with the concatenated topology (high similarity preferred).
262 Then, we mapped filtered transcriptomic reads from nine Zingiberales species and two outgroups
263 to the top 50 most clock-like genes using reads2sam2consensus_baits.py (Vargas et al. 2019),
264 which wraps sam2consensus.py (<https://github.com/edgardomortiz/sam2consensus>). The
265 resulting matrices with *Costus* and non-*Costus* sequences were filtered for those containing all
266 non-*Costus* taxa and reduced by leaving only one sample per monophyletic species. We aligned
267 the 27 resultant gene matrices with MAFFT using the “linsi” algorithm and filtered the
268 alignments for 95% column occupancy with the command “pxclsq” of Phyx (Brown et al. 2017).
269 The filtered 27 alignments were concatenated and analyzed with BEAST v.2.6.1 (Bouckaert et
270 al. 2014) with independent GTR+G models for each gene partition. As a prior, we used a
271 chronogram with relationships fixed based on a Zingiberales phylo-transcriptomic analysis
272 (Carlsen et al. 2018) and our concatenated tree. Branch lengths for the prior tree were calculated
273 with IQ-Tree and later parameterized with TreePL (Smith and O’Meara 2012). Calibrations
274 points were set as follows: 69 Mya (CI = 63–76) to the stem node of the Zingiberaceae based on
275 the fossil *Zingiberopsis magnifolia* (Hickey and Peterson, 1978), and 77 Mya (CI = 69–86) to the
276 crown clade of the Zingiberales based on *Spirematospermum chandlerae* (Friis 1988). Using a
277 birth-death model, BEAST was set to run for 100 m generations sampling every 1 k. We
278 calculated the chronogram after combining 6 sets of 2500 trees from independent runs with
279 LogCombiner v.2.6.1, inputting those in TreeAnnotator v.2.6.1 (Bouckaert et al. 2014) after
280 checking for chain convergence and a minimum effective sample size of 200 for all parameters

281 with Tracer 1.7.1 (Rambaut et al 2014). We used FigTree v1.4.4
282 (<https://github.com/rambaut/figtree/releases>) and ggtree to produce the tree figures (Yu et al.
283 2017).

284 **BIOGEOGRAPHIC ANALYSIS**

285 To test whether early ancestors of *Costus* originated in the mountains or lowlands, we
286 inferred the biogeographic history of the group. We first scored the absence and presence of
287 extant species in four bioregions, Central America + Choco (C), West Indies (W), Andean (A),
288 and Amazonian (M), based on our curated occurrence dataset. We then performed an ancestral
289 range reconstruction using the dispersal-extinction-cladogenesis model (DEC; Ree and Smith
290 2008), a likelihood version (DIVALIKE) of the dispersal-vicariance model (Ronquist 1997), and
291 a likelihood implementation (BAYAREALIKE) of the BAYAREA model (Landis 2013) as
292 implemented in BIOGEOBEARS (Matzke 2013). We abstained from using the founder J
293 parameter given its caveats (Ree and Sanmartín 2018). BIOGEOBEARS infers ancestral areas
294 using the aforementioned models and compares them based on likelihoods. Bioregions were
295 modified from a previous biogeographic study of the Neotropical region (Morrone 2014),
296 considering the distribution of *Costus*. Our input tree was the chronogram inferred after time
297 calibration analysis. The most likely reconstruction was selected based on the corrected Akaike
298 Information Criterion (AICc).

299 **ESTIMATING CLIMATE NICHE**

300 To estimate the climate niche of each species, we obtained four variables representing
301 aspects of temperature and precipitation (<http://www.worldclim.org/>): mean annual temperature,
302 mean annual precipitation, temperature seasonality, and precipitation seasonality. All data were
303 projected into a South America Albers Equal Area Conic projection and resampled to a 1 km x 1

304 km grid cell size. Realized niche position of each species was estimated by circumscribing each
305 species' occurrence-based niche relative to all occupied niche space across Neotropical *Costus*
306 using the "PCA-env" ordination technique implemented in the Ecospat package (Broennimann et
307 al. 2012; Broennimann et al. 2018). Here, the dimensions of the environmental space for *Costus*
308 were reduced to the first and second axes from a principal components analysis (PCA). The PCA
309 of the four climate variables was constructed using all curated Neotropical *Costus* occurrences,
310 subsampled to one occurrence per grid cell (N=2743 grid cells total). We then created a grid with
311 100 x 100 PCA unit grid cells and used the species' presence data to project the density of each
312 species into environmental space using a kernel density function (Broennimann et al. 2012).
313 Niche position for each species was estimated as the mean of PC1 and PC2.

314 To determine whether mountain-influenced taxa occupy a larger volume of climate niche
315 space overall, we tested whether the variation in species' mean niche values differ by region.
316 Species were categorized as either Amazonian (all occurrences contained in the Amazon and/or
317 West Indies bioregions) or mountain-influenced (occurrences fully or partially contained in the
318 Central America + Choco or Andean bioregions). We visualized the evolution of climate niches
319 by projecting the phylogeny on species' mean values for PC1 and PC2 using Phytools (Revell
320 2012), and we used Levene's tests on PC1 and PC2 separately to compare the variance in mean
321 niche values between regions (leveneTest function, car package in R, Fox and Weisberg 2019).

322 **EVOLUTION OF POLLINATION SYNDROMES**

323 We evaluated whether hummingbird pollination and/or shifts from orchid bee to
324 hummingbird pollination are more prevalent in mountain-influenced than Amazonian taxa.
325 Orchid bee- or hummingbird-pollination syndromes were assigned to taxa based on previous
326 studies in the genus (Maas 1972; Maas 1977; Kay and Schemske 2003; Kay et al. 2005) and

327 KMK expertise. Although only a subset of species has pollination data, pollination syndromes
328 accurately predict whether orchid bees v. hummingbirds are the primary pollinator (Kay and
329 Schemske 2003). Thus, pollination syndromes serve as a tractable proxy for an important biotic
330 interaction that could contribute to ecogeographic divergence. We first used a chi-squared test to
331 determine whether hummingbird pollination is more frequent among mountain-influenced
332 species than Amazonian species, regardless of their phylogenetic history. To account for
333 phylogenetic history, we used Pagel's (1994) test to determine whether there was correlated
334 evolution of pollination syndrome and geographic region (function `fitPagel`, `phytools` package,
335 Revell 2012; although see Maddison and FitzJohn 2015 for caveats regarding this method). We
336 then performed a character reconstruction of pollination syndromes on the phylogeny (function
337 `make.simmap`, `phytools` package; Revell 2012) and used another chi-squared test to determine
338 whether reconstructed shifts from bee to hummingbird pollination are more likely in mountain-
339 influenced vs. Amazonian ancestors. Ancestors were categorized based on the biogeographic and
340 pollination character state reconstructions.

341 **IDENTIFYING SISTER TAXA**

342 We identified sister taxa for comparisons of range overlap, climate niche divergence, and
343 pollination shifts in recent and phylogenetically independent speciation events. Sister taxa were
344 identified from the 1000 rapid bootstraps of the concatenated alignment by first pruning the trees
345 to the reduced taxon set used for the time-calibrated phylogeny and then counting the frequency
346 of all sister pairs across bootstrap replicates with a custom R script (R Core team 2020). This
347 frequency was used as a weighting factor in downstream analyses to account for uncertainty in
348 tree topology. Sister pairs were categorized as either mountain-influenced (one or both species
349 occurred in Central America, Choco, or the Andes) or as Amazonian (both species occurred in

350 the lowland Amazon, or one species in the Amazon and the other in the West Indies). We
351 flagged potential cases of budding speciation in the phylogeny when we observed a widespread
352 species having a taxon nested in it with a smaller range area; we arbitrarily chose a minimum
353 asymmetry ratio of 5 (large / small range) as a cut off.

354 **ESTIMATING SISTER PAIR RANGE OVERLAP, RANGE ASYMMETRY, AND** 355 **CLIMATIC NICHE DIVERGENCE**

356 For each sister pair, we used the filtered occurrence data to estimate the degree of range
357 overlap using a grid approach. We divided the Neotropics into a series of cells by grid lines that
358 follow degree longitude and latitude using the “raster” R package version 2.9-5 (Hijmans 2016).
359 We calculated range overlap as the summed area of grid cells occupied by both species, divided
360 by the summed area of occupied grid cells for the smaller ranged species. Thus, range overlap
361 could range between 0 (no range overlap) and 1 (the smaller-ranged species is found only within
362 the range of the larger-ranged species) (Barraclough and Vogler 2000; Fitzpatrick and Turelli,
363 2006). We calculated range size asymmetry as the summed area of grid cells occupied by the
364 larger ranged species divided by the summed area of grid cells for the smaller ranged species
365 (Fitzpatrick and Turelli 2006). In order to assess whether the ensuing analyses were sensitive to
366 spatial scale, range overlap and size asymmetry were calculated at two cell sizes, 0.05 and 0.1
367 decimal degrees, representing grid cells of approximately 33 and 131 km² respectively (exact
368 value varies by latitude). Sister pairs lacking adequate geographic data (fewer than 4 known
369 occurrences for one or both species) and those taxonomically poorly understood were excluded
370 from all downstream analyses (Table S4).

371 **COMPARING MOUNTAIN-INFLUENCED AND AMAZONIAN SISTER PAIRS**

372 We performed a series of analyses to determine whether climate divergence or
373 geographic isolation differs between mountain-influenced and Amazonian sister pairs. We
374 predicted that mountain-influenced pairs would have greater niche divergence and/or greater
375 geographic isolation (less range overlap), and more frequent budding speciation than Amazonian
376 pairs. We also predicted that mountain-influenced pairs would have more frequent shifts to
377 hummingbird pollination than Amazonian pairs, but were unable to make this comparison with
378 only sister pairs because of the small number of shifts occurring at the tips of the phylogeny.

379 To compare climate niche divergence between regions, we compared the frequency of
380 climate niche equivalency and the degree of climate niche divergence for mountain-influenced v.
381 Amazonian sister pairs. To estimate climate niche equivalency, we determined whether each
382 sister pair occupies statistically equivalent niches, i.e., that the niche overlap between sister
383 species is equal to that of two species occupying random niches in the same range of
384 environmental conditions that are available to the species in question (Warren et al. 2008;
385 Broennimann et al. 2012). This was performed using the function `ecospat.niche.equivalency.test`
386 (`ecospat` package, Broennimann et al. 2018), whereby the observed overlap is compared to a null
387 distribution of simulated overlaps when randomly reallocating the occurrences of both species
388 among the joint distribution of occurrences. Only pairs where each member species occupied at
389 least 5 grid cells were used in this analysis (N=22 sister pairs). The frequency of climate niche
390 equivalency was compared between regions (mountain-influenced, Amazonian) with a weighted
391 chi-squared test, weighted by the number of bootstrapped trees containing a given sister pair
392 (function `wtd.chisq`, `weights` package, Pasek 2020). To compare the mean climate niche
393 divergence of sister pairs between regions, we calculated climate niche divergence for each pair

394 as the euclidean distance between mean PC1 and PC2 for each species and then used a two
395 sample T-test, weighted by the number of bootstrapped trees containing a given sister pair
396 (wtd.t.test function, weights package, Pasek 2020).

397 To compare geographic isolation between regions, we first quantified the current range
398 overlap for sister pairs between regions and then examined how range overlap varies with
399 divergence time. To compare the mean current range overlap, we used a two sample T-test,
400 weighted by the number of bootstrapped trees containing a given sister pair (wtd.t.test function,
401 weights package, Pasek 2020). We note that current overlap may differ from overlap at the time
402 of speciation due to post-speciation range expansions, contractions and shifts; however, by using
403 only sister species and comparing regions, we can infer differences in geographic isolation
404 between regions for the most recently diverged species pairs in *Costus*.

405 To determine whether allopatric speciation is more prevalent in the mountains, we tested
406 whether sister pair range overlap was predicted by divergence time, region, and their interaction
407 using a linear model (lm function, weighted by the number of bootstrapped trees containing a
408 given sister pair, R). If allopatric speciation is dominant, then more recently-diverged species
409 pairs should be allopatric, whereas older pairs might show range overlap due to range shifts since
410 speciation (Fitzpatrick and Turelli 2006). Contrastingly, if parapatric speciation is dominant,
411 younger sister species pairs should show range overlap whereas older pairs should show a variety
412 of configurations (Fitzpatrick and Turelli 2006; Anacker and Strauss 2014). A significant
413 interaction between divergence time and region would indicate that the predominant geographic
414 mode of speciation differs by region.

415 Finally, to determine whether budding speciation occurs and whether this phenomenon
416 varies by region, we examined the relationship between range asymmetry and divergence time,

417 and we also looked for evidence of nested phylogenetic relationships that would indicate a small-
418 ranged taxon was derived from within a widespread progenitor taxon. We first tested whether
419 sister pair range asymmetry was predicted by divergence time, region, and their interaction using
420 a generalized linear model with a natural log link function, gamma distribution suitable for left-
421 skewed response variables such as range size asymmetry (glm function, weighted by the number
422 of bootstrapped trees containing a given sister pair). If budding speciation is common, then range
423 size asymmetry is predicted to be greatest for the youngest sister pairs and to decrease on
424 average with time, as ranges undergo expansion or contraction following the initial budding
425 speciation event (Fitzpatrick and Turelli 2006; Grossenbacher et al. 2014). A significant
426 interaction between divergence time and region would indicate that the signature of budding
427 speciation differs by region. Significance of predictors was assessed by likelihood ratio chi-
428 squared tests (LR) using single term deletions. Our phylogenetic sampling also allowed us to
429 assess nested phylogenetic relationships indicative of budding speciation in four putative cases,
430 three mountain-influenced and one Amazonian (*C. scaber* in Central America – *C. ricus*, *C.*
431 *pulverulentus* – *C. sp. nov.* 18020/18049, *C. laevis* – *C. wilsonii*, and *C. scaber* in South America
432 – *C. spicatus*, respectively). We did not know in advance which, if any, species were produced
433 by budding speciation, but we attempted to sample across the known geographic distributions of
434 multiple widespread taxa.

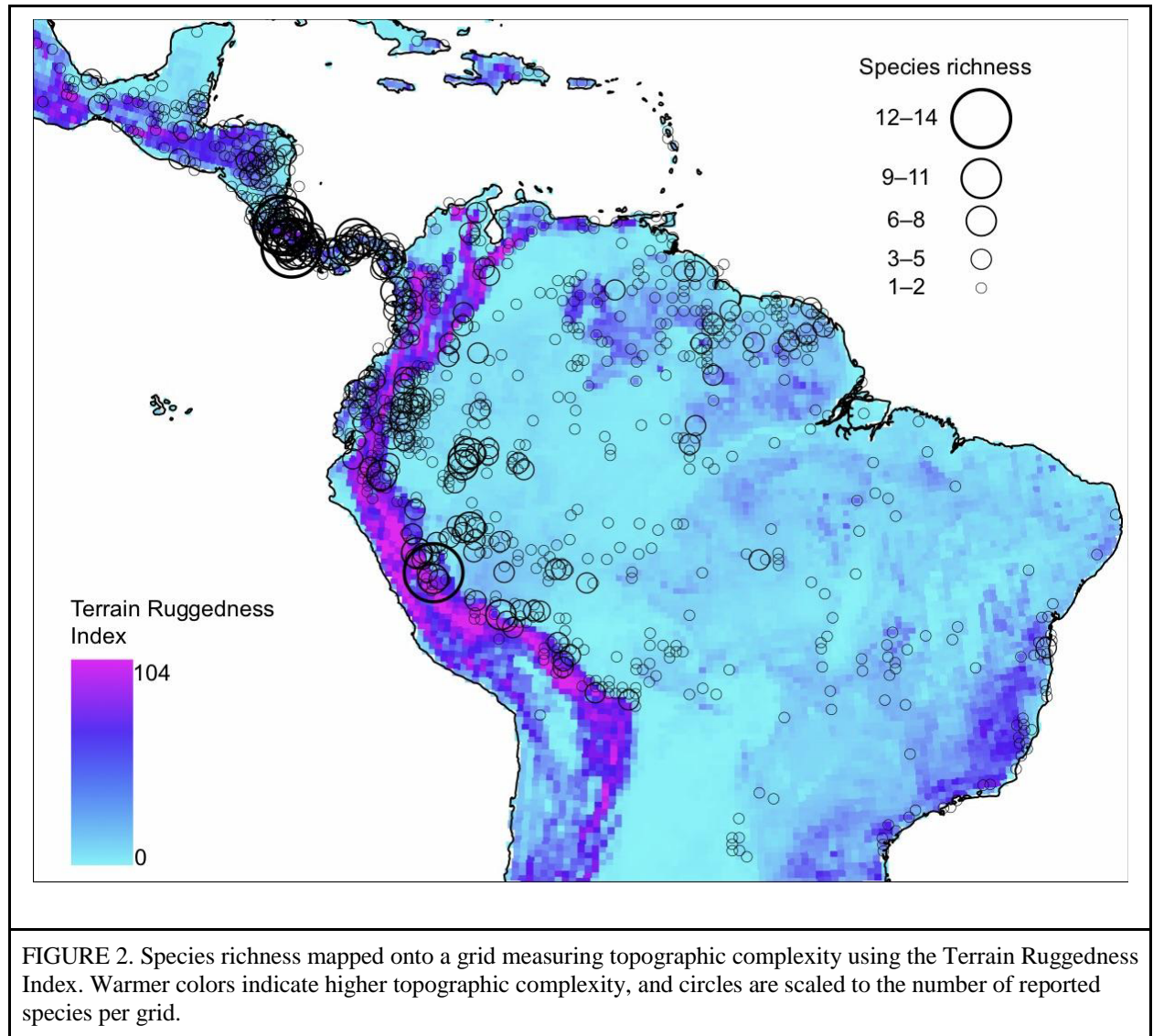
435 Because we only have a modest set of sister pairs that are used repeatedly in the analyses
436 above, we present exact p-values and describe effect sizes, without using a strict $\alpha = 0.05$ to
437 determine significance.

438 *Results*

439 **Topographic complexity and species richness**

440 We find a positive association between topographic complexity and species richness in
441 *Costus*, consistent with mountains playing a key role in diversification of this clade (Fig. 2). We
442 recover a significant spatial autocorrelation between Terrain Ruggedness Index (TRI) and
443 species richness (Fig. 2; Moran's $I > 0.12$, $P < 0.001$, across both spatial scales). Ordinary least
444 squares regression shows a significant positive relationship between TRI and species richness
445 (1600 km^2 , $F = 7.56_{1,973df}$, $P = 0.006$; 6400 km^2 , $F = 6.82_{1,597df}$, $P = 0.009$). Simultaneous
446 Autoregressive (SAR) lag models also shows a positive relationship between TRI and species
447 richness, however, significance varies by scale (1600 km^2 , $z=1.89$, $P = 0.138$, pseudo-r squared =
448 0.227 ; 6400 km^2 , $z = 1.89$, $P = 0.049$, pseudo-r squared= 0.246). SAR lag models are favored
449 over ordinary least squares regression using AIC (1600 km^2 , Likelihood Ratio = 1282.51 , $P <$
450 0.001 ; 6400 km^2 , Likelihood Ratio = 170.55 , $P < 0.001$). Overall, *Costus* shows a center of
451 species richness in the Central America + Choco and the northern Andean floristic regions,
452 moderate richness in the Guiana Shield and the eastern slope of the southern Andes, and
453 relatively low richness in the Amazon basin. It is important to note that our sampling relied on
454 collection efforts carried out by previous collectors and our team, which largely focused on
455 sampling Central America, and therefore it is possible that Andean and Amazonian *Costus*
456 diversity is underestimated. Finally, after accounting for uneven sampling between regions using
457 rarefaction, we find that richness is significantly greater in mountainous than lowland regions
458 (mean rarefied richness = 55.6 and 40.3 species respectively and 95% confidence intervals are
459 non-overlapping, Fig. S1).

460



461

462 **Phylogenetic analysis**

463 We infer a robust species-level phylogeny for *Costus*. Our concatenated matrix has
464 95.3% cell occupancy comprising 133 samples by 756 genes in 1,474,816 aligned columns
465 (Tables S5–6). Average length per gene, including partial introns, is 1,951 bp. Samples have an
466 average of 728 genes. We calculate two species trees, the first based on a concatenated alignment
467 and a second based on individual gene trees in a coalescent framework. Both species trees have
468 robust support and similar topologies (Figs. 3,S2). Because of the general low molecular

469 divergence found in the ingroup (average pairwise identity = 90.0%) and the low signal found in
470 individual genes (Fig. S3), we selected the concatenated topology as the best phylogenetic
471 hypothesis for the remainder of this study (Fig. 3). Our *Costus* phylogeny is robust with most
472 nodes presenting full or high support (≥ 95 ultrafast bootstrap, ≥ 90 Shimodaira-Hasegawa
473 approximate likelihood ratio test) and generally agrees with previous phylogenetic studies in
474 *Costus* (Kay et al 2005, André et al 2016).

475 **TIME-CALIBRATION OF THE PHYLOGENY**

476 Our time-calibrated phylogeny dates the crown clade of Neotropical *Costus* to 3.0 Mya
477 with a 95% CI = 1.50–4.87 (Fig. 4). Our matrix for the calculation of the chronogram, which
478 included Zingiberales sequences for each one of its families and a reduced *Costus* sampling, is
479 composed of 69 taxa by 27 clock-like genes, comprising 22,237 aligned columns (Table S7). Our
480 time-estimation for the origin of *Costus* in the Neotropics is consistent with a previous dating of
481 1.1–5.4 Mya (Kay et al. 2005) but younger than another of ~7 Mya (André et al. 2016).

482 **BIOGEOGRAPHIC ANALYSIS**

483 Ancestral range reconstruction suggests that the Central American region has dominated
484 the biogeographical history of the genus in the Neotropics (Fig. 4). Based on AICc, the model
485 that best fits the reconstruction is DIVALIKE (AIC = 185.5), followed by DEC (AIC = 188.2),
486 and BAYAREALIKE (AIC = 230.5). The DIVALIKE reconstruction shows that nearly half of
487 the ancestors in the phylogeny were distributed in Central America (25 out of 54 ancestors with a
488 > 0.90 probability) with the vast majority of the early ancestors estimated as Central American.
489 Colonization out of Central America is inferred to have happened around 1.5 Mya to the Andean
490 and the Amazon regions. Similar biogeographical patterns are also found in the reconstruction
491 inferred with the DEC but not BAYAREALIKE models (Figs. S4,S5).

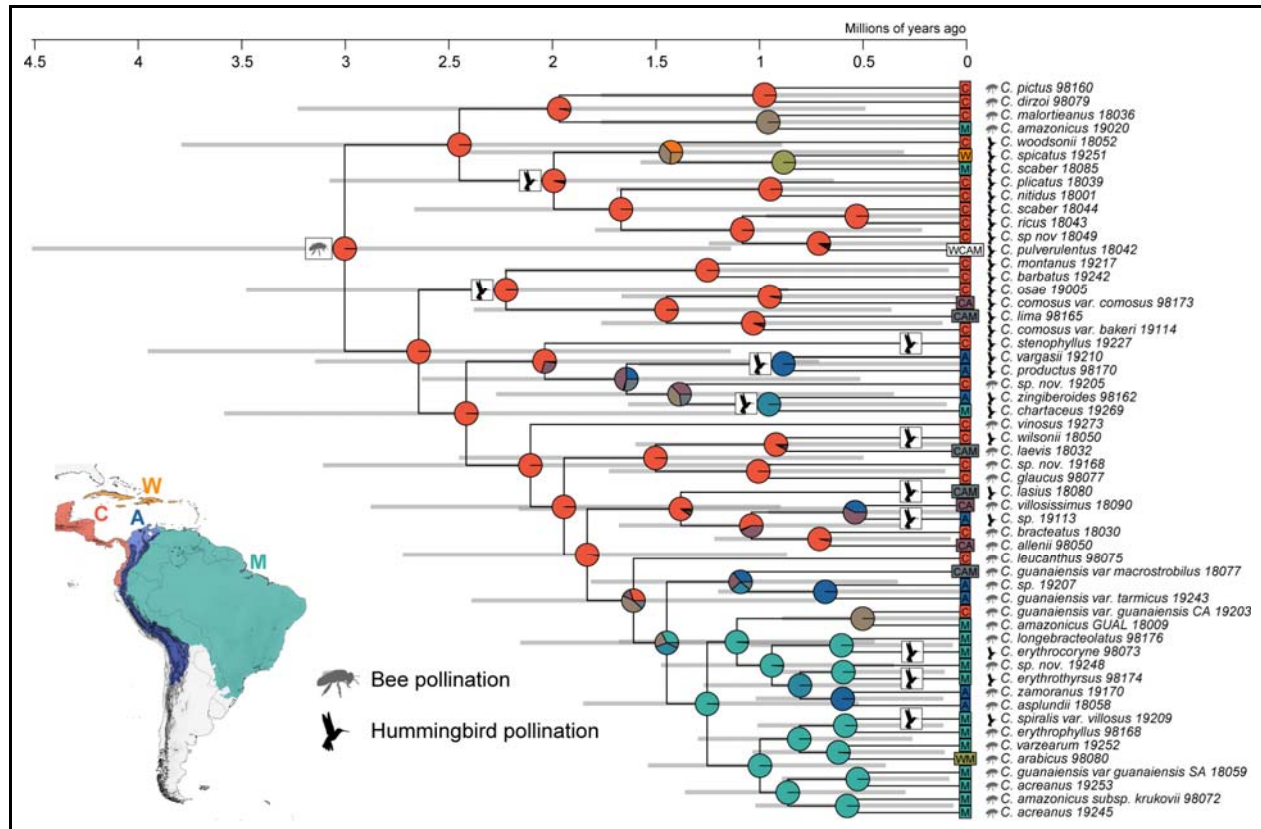


FIGURE 4. Time calibrated phylogeny, DIVALIKE biogeographic historical inference, and ancestral pollination character reconstruction for Neotropical *Costus*. Pie charts represent percent probabilities of areas for the ranges of ancestors. C: Central America and/or Choco, W: West Indies, A: Andes, M: Amazon. Mixed colors indicate combined bioregions. Pollination syndromes are indicated for every tip taxon along with inferred transitions from bee to hummingbird pollination on internal branches. The most recent common ancestor is reconstructed as bee pollinated. Gray horizontal bars represent 95% confidence intervals for node ages.

493

494 CLIMATE NICHE OF MOUNTAIN-INFLUENCED AND AMAZONIA SPECIES

495 Principal component analysis reveals the first two climate niche axes explain 42 and 23%

496 of the variation among all *Costus* occurrences, respectively. PC1 primarily describes variation in

497 mean annual precipitation and seasonality: low values indicate greater precipitation and high

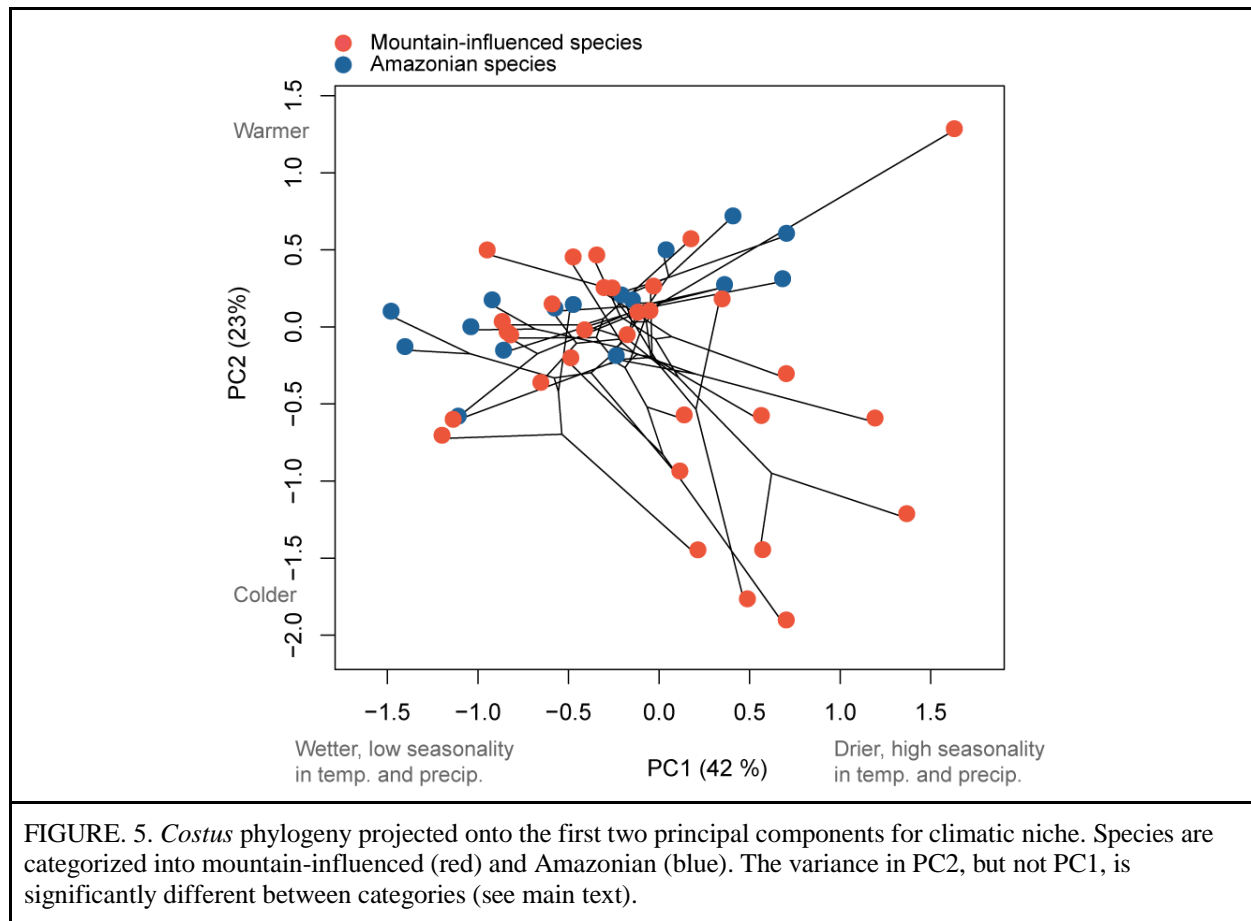
498 values indicate higher seasonality in both temperature and precipitation. PC2 primarily describes

499 variation in mean annual temperature: low values indicate cooler environments. Overall, we

500 found that the variance in species' mean niche values was greater among mountain-influenced

501 than among Amazonian species for PC2 (Fig. 5; PC2 $F = 10.05^{1,46df}$, $P = 0.003$), but not PC1

502 (Levene's test: PC1 $F = 0.05^{1,46df}$, $P = 0.824$), indicating that, together, mountain influenced taxa
503 are occupying a larger temperature niche space.



504

505 **EVOLUTION OF POLLINATION SYNDROMES IN MOUNTAINS VERSUS THE** 506 **AMAZON**

507 The most likely scenario for the evolution of pollination syndromes in our phylogeny
508 involves 11 shifts from orchid bee- to hummingbird-pollination, with seven shifts happening in
509 recent divergence events and four along internal branches of the phylogeny. We find no
510 significant difference in the proportion of hummingbird-pollinated taxa between mountain-
511 influenced and Amazonian taxa (21 out of 39 taxa v. 5 out of 16 taxa; $X^2(1, N = 55) = 1.51$, $P =$
512 0.220; Fig. S6A). We find no evidence of correlated evolution of pollination syndrome and

513 geographic region (Pagel's test, $LR = 0.38$, $P = 0.984$). Similarly, we find no significant
514 difference in the frequency of shifts to hummingbird pollination in ancestors characterized as
515 mountain-influenced or Amazonian (8 shifts along 81 branches v. 3 shifts along 28 branches; X^2
516 (NA, $N = 109$) = 0.02, $P = 1$; Fig. S6B).

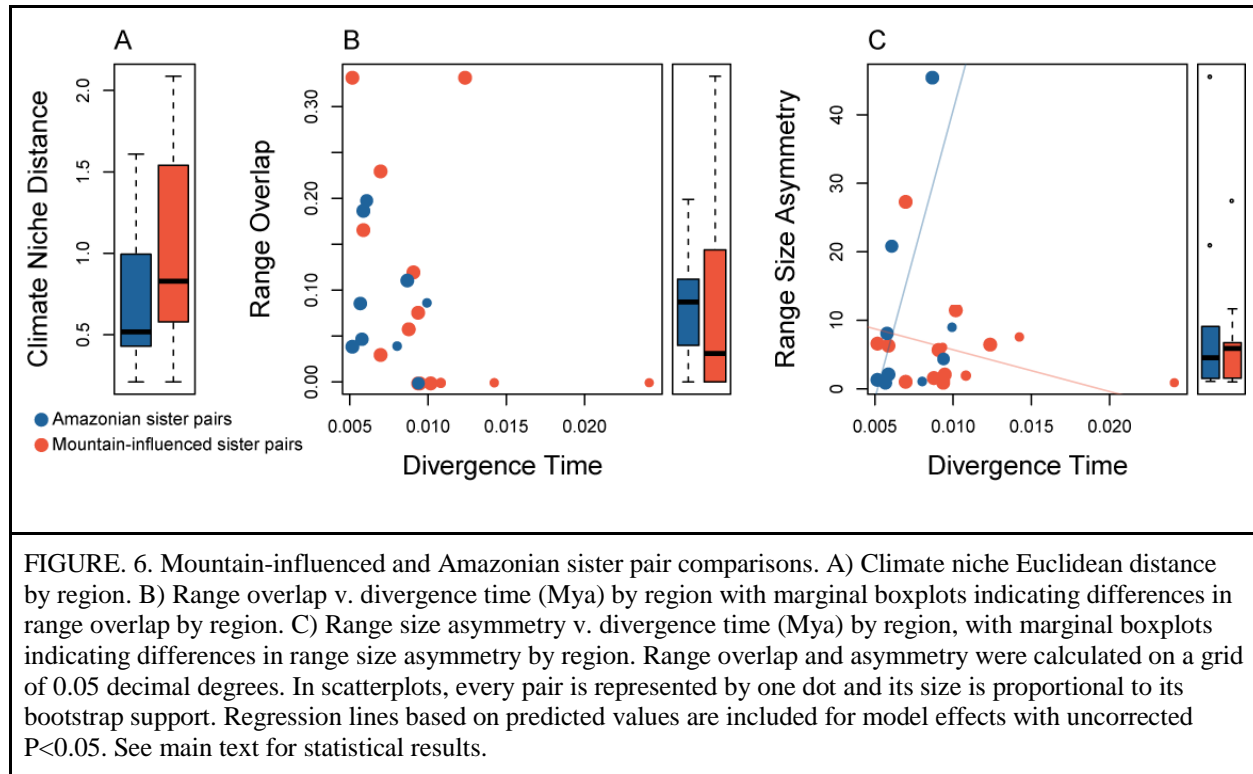
517 MOUNTAIN-INFLUENCED AND AMAZONIAN SISTER PAIR COMPARISON

518 Climate niche divergence does not differ between pair types. Thirty-one sister pairs were
519 inferred from the bootstrap replicates of the phylogenetic analysis, and 24 have enough
520 geographic and taxonomic information for comparative analyses (Table S4, Fig. S7). Of these,
521 15 pairs are identified as mountain-influenced and 9 pairs as Amazonian. We test for niche
522 equivalency for 22 out of our 24 pairs (2 taxa have less than 5 occurrences) rejecting niche
523 equivalency for 60% of sister pairs (Table S4, Fig. S8). We find no difference in the proportion
524 of mountain-influenced and Amazonian pairs with equivalent niches ($X^2(1, N=22) = 14.29$, $P =$
525 0.217). Climatic niche divergence is on average 46% greater for mountain influenced pairs
526 relative to Amazonian pairs; however, this difference is not significant (weighted t-test, $t = -$
527 $1.47^{20.df}$, $P = 0.157$; Figs. 6, 7).

528 We find no support for the hypothesis that range overlap differs in the mountains versus
529 lowlands. Overall, there is generally little range overlap for sister pairs and no evidence that
530 range overlap varies by region. Average range overlap is 0.09 for mountain influenced and
531 Amazonian pairs at the fine spatial scale (weighted t-test, $t = -0.56^{22.df}$, $P = 0.584$; Figs. 6, 7).
532 Range overlap is not predicted by divergence time, region, or their interaction (Fig. 6; linear
533 model: divergence time $F = 0.50^{1,20.df}$, $P = 0.487$; region $F = 0.78^{1,20.df}$, $P = 0.386$; divergence time
534 by region $F = 0.006^{1,20.df}$, $P = 0.937$). We note that there are two outlier data points with range
535 overlap >0.3 (*C. montanus* – *C. barbatus*, *C. ricus* – *C. scaber*), breaking model assumptions.

536 When those points are removed from the analysis, range overlap decreases with divergence time,
537 consistent with parapatric speciation, but is not predicted by region or their interaction
538 (divergence time $F = 6.63^{1,18df}$, $P = 0.019$; region $F = 0.44^{1,18df}$, $P = 0.515$; divergence time by
539 region $F = 1.35^{1,18df}$, $P = 0.261$). We urge caution interpreting this result, since there is no
540 biological justification for excluding the two outliers.

541 We find limited support for a budding model of speciation being more common in the
542 mountains than lowlands. Range size asymmetry is greater for younger relative to older
543 mountain-influenced pairs, while the opposite is observed for Amazonian pairs (Fig. 6; GLM:
544 divergence time $X^2 = 0.039$, $P = 0.843$; region $X^2 = 1.747$, $P = 0.186$; divergence time by region
545 $X^2 = 4.34$, $P = 0.037$). In light of multiple comparisons between sister pair types, we treat this
546 result with caution. Note that we present only range overlap and asymmetry results for the fine
547 spatial scale above (~33 km²). Results at the coarse spatial scale were qualitatively similar for all
548 tests (Fig. S9). Finally, we assess evidence for nested phylogenetic relationships between four
549 taxon pairs, three mountain-influenced and one Amazonian (*C. scaber* in Central America – *C.*
550 *ricus*, *C. pulverulentus* – *C. sp. nov.18020/18049*, *C. laevis* – *C. wilsonii*, and *C. scaber* in South
551 America – *C. spicatus*, respectively). The first two of those pairs show paraphyly consistent with
552 budding speciation, whereas the latter two are reciprocally monophyletic, although they all show
553 substantial range asymmetry (Fig. 2, Table S4).



554 Discussion

555 Mountains are associated with exceptionally high plant diversity in the Neotropics, with
556 tree species richness peaking in the forests nestled at the eastern base of the Northern Andes (ter
557 Steege et al. 2010) and some of the fastest known plant radiations on earth occur in high
558 elevation Neotropical habitats (Drummond et al. 2012; Madriñán et al. 2013, Uribe-Convers and
559 Tank 2015, Lagomarsino et al. 2016; Vargas et al. 2017, Contreras-Ortiz et al. 2018; Morales-
560 Briones et al. 2018). We see a similar pattern in Neotropical *Costus*, with species richness
561 positively correlated with topographic complexity across its geographic range in Central and
562 South America.

563 Despite the important contribution of tropical mountains to the latitudinal diversity
564 gradient, the mechanisms underlying this pattern remain unclear. Gentry (1982) hypothesized
565 that recent mountain uplift in the Andes and southern Central America promoted rapid

566 diversification of plants with short generation times (e.g., herbs, shrubs, vines and epiphytes) by
567 providing strong ecogeographic gradients in both climate and pollinators, especially
568 hummingbirds. In contrast, Janzen (1967; reviewed in Sheldon et al. 2018) proposed that the lack
569 of strong temperature seasonality in the tropics leads to narrow physiological tolerances and
570 greater potential for allopatric speciation due to topographic dispersal barriers in mountains. The
571 relative importance of these two mechanisms in driving species richness is unclear—
572 investigation requires understanding species-level relationships in clades that span both montane
573 and lowland environments, and until now we have generally been left comparing Amazonian
574 trees (e.g., Fine et al. 2005; Vargas and Dick 2020) to high elevation shrubs and herbs (e.g.,
575 Contreras-Ortiz et al. 2017; Vargas and Simpson 2019). *Costus* provides an opportunity to use a
576 species-level phylogeny to examine possible speciation mechanisms in a clade that spans
577 lowlands to cloud forests, albeit for a single herbaceous life form.

578 We first examine ecogeographic divergence caused by macroclimatic conditions and
579 adaptation to different functional groups of pollinators: orchid bees and hummingbirds. We find
580 that both mountain-influenced and Amazonian pairs experience climate niche divergence at
581 similar frequencies (Fig. 6. Table S4), with only a marginal trend of greater climatic niche
582 divergence in mountain-influenced pairs, a remarkable result given the steep gradients in climate
583 in tropical mountains. Nevertheless, montane species occupy a significantly greater amount of
584 climatic niche space overall, primarily due to expansion into cooler environments (Fig. 5). Taken
585 together, our results suggest that climatic divergence occurs in both mountain-influenced and
586 Amazonian pairs, and that mountain-influenced taxa occupy the greater temperature variation the
587 mountains offer (Rahbek et al. 2019a). Despite hummingbird pollination being common in
588 mountain-influenced species, it is not proportionally more common than in Amazonian species.

589 Moreover, we observe similar proportions of pollination shifts throughout the tree when
590 ancestors are categorized as mountain-influenced or Amazonian based on our biogeographic
591 reconstruction (Fig. 4,S6). Thus, while hummingbird pollination may be an important driver of
592 diversification in the mountain-influenced pairs, our results show that it is similarly important in
593 lowland Amazonian pairs.

594 If mountains serve as dispersal barriers and cause long-lasting allopatric separation, we
595 predicted that mountain-influenced pairs would have less range overlap than Amazonian pairs .
596 We find instead that there is generally little range overlap for sister species, regardless of
597 whether they are mountain-influenced or Amazonian (Fig. 6). Although slightly more mountain-
598 influenced than Amazonian pairs have complete allopatric separation (e.g., *C. amazonicus* – *C.*
599 *malortieanus*; Fig. 7, right panel), there is no significant difference between regions. This result
600 may simply reflect the importance of geographic isolation for most, if not all, speciation. Our
601 results contrast with a previous study in *Costus*, which used species distribution models to
602 predict co-occurrence across all nodes in the phylogeny and found extensive sympatry (André et
603 al. 2016). Species distribution models may lead to dramatic overestimates of actual co-
604 occurrence (Guisan and Rahbek 2011), particularly in topographically complex landscapes
605 where dispersal is likely limited. Furthermore, because geographic signatures of speciation erode
606 over time as ranges expand, contract, and shift (Fitzpatrick and Turelli 2006), the use of sister
607 species comparisons, rather than all nodes in the phylogeny is more likely to yield information
608 regarding speciation itself.

609 Additionally, we examined evidence for budding speciation, which may be common
610 when speciation is driven by topographic dispersal barriers (Anacker and Strauss 2014;
611 Grossenbacher et al. 2014). Indirect evidence of budding speciation could come from range size

612 asymmetry decreasing over time-since-divergence, since derivative species should start from
613 small marginal populations. We find a weak pattern of this being the case in mountain-
614 influenced, but not Amazonian pairs (Fig. 6C). Further evidence for budding speciation could
615 come from geographically intensive phylogenetic sampling of sister pairs showing that the
616 smaller-ranged species is nested within the widespread, paraphyletic progenitor (Baldwin 2005).
617 While we find support for this pattern in two mountain-influenced pairs, our phylogenetic
618 sampling was not extensive enough to make statistical comparisons with Amazonian taxa. Thus,
619 while budding speciation likely occurs in *Costus*, our results are not sufficient to draw robust
620 conclusions about the prevalence of budding speciation in the mountains or differences in the
621 frequency of budding speciation between regions. In that sense, our results contrast with the clear
622 patterns of budding speciation found in other plant and animal biodiversity hotspots (Anacker
623 and Strauss 2014; Grossenbacher et al. 2014; Gaboriau et al. 2018).

624 We see examples of how climatic niche divergence, range overlap and asymmetry, and
625 pollination shifts can occur in both mountain-influenced and Amazonian pairs (Fig. 7). *Costus*
626 *laevis* is a widespread bee-pollinated lowland species whose range abuts its restricted (but not
627 phylogenetically nested) montane hummingbird-pollinated sister, *C. wilsonii*, in southern Costa
628 Rica. In this case, speciation may be explained by upslope adaptation to a colder drier
629 environment accompanied by a shift to hummingbird pollination in *C. wilsonii*, perhaps the
630 quintessential ecological specialization model of divergence that Gentry (1982) envisioned for
631 Neotropical mountains (Fig. 1E; Fig. 7 center). In contrast, the lowland Amazonian pair *C.*
632 *erythrophyllus* – *C. spiralis* shows comparable levels of range overlap, range asymmetry and
633 climate niche divergence, in this case along PC1 (precipitation and seasonality) rather than PC2
634 (temperature), as well as a shift in pollination syndrome, but without the direct influence of

635 mountains (Fig. 7 left panel). These examples illustrate that multiple ecogeographic factors can
636 promote lineage splitting in both mountains and lowlands.

637 How can the similarity in patterns of speciation between mountain-influenced and
638 Amazonian pairs be reconciled with the pattern of increased species richness in mountainous
639 regions we see in *Costus*? This pattern could be driven by other factors contributing to higher
640 rates of diversification in mountainous regions, such as less extinction or more immigration, or to
641 differences in the amount of time *Costus* has spent in mountainous v. lowland regions. Our
642 biogeographic reconstructions suggest the latter—*Costus* likely first established ca. 3 Mya in
643 Central America when the Talamanca Cordillera started to uplift (Driese et al. 2007), and the
644 genus diversified in this region for close to 1.5 My before colonizing the already elevated Andes
645 cordillera (Gregory-Wodzicki 2000) and the Amazon lowlands (Fig. 4). Although we were
646 unable to directly compare diversification rates due to our sample size of species and transitions
647 between regions (Maddison and Fitzjohn 2015), we find that Amazonian sister pairs are
648 significantly younger than mountain-influenced pairs (Fig. S9A). This difference is consistent
649 with the Amazon basin as a region of recent and rapid diversification, and counters the
650 alternative hypothesis of higher rates of diversification in mountainous regions. In general,
651 *Costus* has had more time to diversify in Central America and northwestern South America than
652 in the Amazon basin, without the need for invoking different modes or rates of speciation.

653 To what extent are our results likely to apply to other Neotropical plant lineages? The
654 role of mountains in the diversification of *Costus*, which is restricted to < ca. 2000 m, may be
655 different from higher elevation tropical montane lineages. Studies of Andean paramo plant
656 groups, which occur on mountain tops above treeline, have found substantial allopatry
657 (*Espeletia*: Diazgranados and Barber 2017; *Linochilus*: Vargas and Simpson 2019) and

658 ecological divergence (Campanulaceae: Lagomarsino et al. 2016; *Lupinus*: Nevado et al. 2016,
659 *Espeletia*: Cortés et al. 2018). Alternatively, the relatively young geological age of Neotropical
660 mountains, including the Andes and Central American Cordillera, may spur rapid diversification
661 simply through the opening of new niche space (Weir and Schluter 2008) and without any
662 consistent difference in speciation modes. Much of the plant species richness and endemism in
663 Neotropical mountains comprises herbs and shrubs with short generation times that are able to
664 take advantage of open mountain niche space quickly (Gentry 1982). In contrast, Neotropical
665 trees typically have their center of diversity in the Amazon lowlands (Gentry 1982) and these
666 lineages can date back to the Paleocene (Dick and Pennington 2019). Finally, diversification
667 studies of plants in the Amazon have found a large role for edaphic ecological specialization
668 (*Protium*: Fine et al. 2014, Misiewicz and Fine 2014), other fine-scale habitat divergence
669 (Gesneriaceae: Roalson and Roberts 2016), and biotic interactions, (*Pitcairnia*: Palma-Silva et
670 al. 2011, *Ruellia*: Tripp and Tsai 2017). Both abiotic and biotic conditions vary across lowland
671 forests, and speciation may typically involve ecogeographic isolation even without the influence
672 of mountains.

673 Taken together, our study suggests that ecogeographic differentiation and geographic
674 isolation are drivers of speciation in mountainous tropical regions, and that they happen similarly
675 in mountains and tropical lowlands. Although mountains provide a larger overall climate niche
676 landscape (Rahbek et al. 2019a), we find no evidence that speciation modes are fundamentally
677 different. However, we caution that these results may not apply to tropical alpine clades that are
678 able to colonize geologically young and spatially disjunct ecosystems above treeline, and these
679 clades may contribute disproportionately to the species richness and endemism of tropical
680 mountains (Hughes and Atchinson 2015). Further studies with a similar framework to ours are

681 needed to determine whether our conclusions can be generalized across tropical organisms in
682 mountainous and lowland regions. Our study demonstrates the potential of combining species-
683 level phylogenomics with spatial and ecological data to test longstanding hypotheses about
684 diversification in tropical mountains.

685

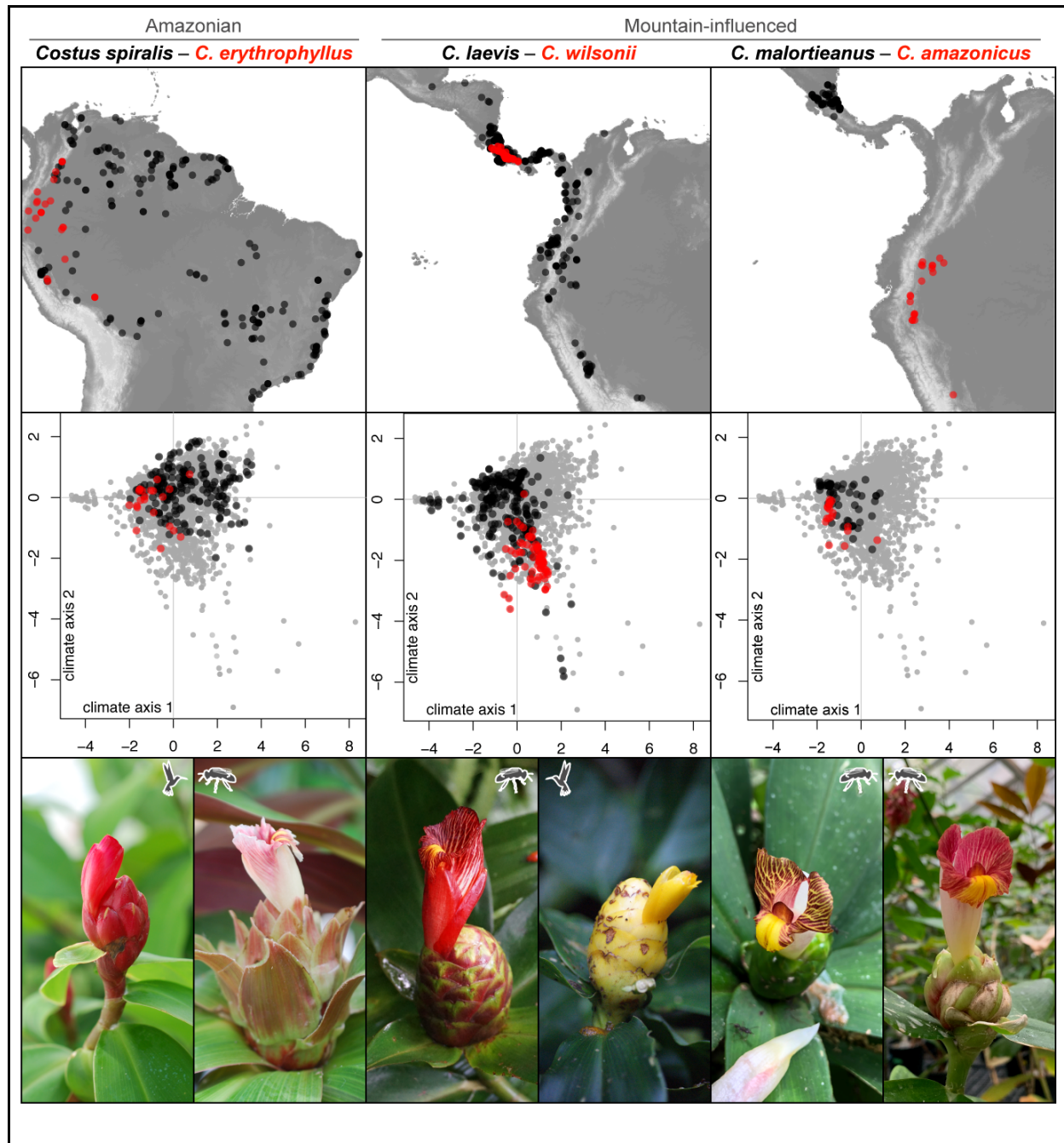


FIGURE 7. Range maps, climate niches, and inflorescence photos of representative sister species pairs. Left: an Amazonian pair. Center and right: mountain influenced pairs. Top row: occurrences in the map. Central row: comparisons between the climate niches of the sister species (PC axes correspond to Fig. 5). Photo credits from left to right: *Costus spiralis* and *C. erythrophyllus* by KMK, *C. laevis* by R. Maguiña, *C. wilsonii* by P. Juarez, *C. malorteanus* by DLG, and *C. amazonicus* by KMK.

686

687 *Literature*

688 Anacker, B. L., and S. Y. Strauss. 2014. The geography and ecology of plant speciation:
689 Range overlap and niche divergence in sister species. *Proc. R. Soc. B Biol. Sci.* 281.

690 André, T., S. Salzman, T. Wendt, and C. Specht. 2016. Speciation dynamics and
691 biogeography of Neotropical spiral gingers (Costaceae). *Mol. Phylogenet. Evol.*
692 103:55–63.

693 Angert, A. L., and D. W. Schemske. 2005. The evolution of species' distributions:
694 reciprocal transplants across the elevation ranges of *Mimulus Cardinalis* and *M. lewisii*.
695 *Evolution.* 59:1671.

696 Angert, A. L., H. D. Bradshaw, and D. W. Schemske. 2008. Using experimental evolution
697 to investigate geographic range limits in monkeyflowers. *Evolution.* 62:2660–2675.

698 Baldwin, B. G. 2005. Origin of the serpentine-endemic herb *Layia discoidea* from the
699 widespread *L. glandulosa* (Compositae). *Evolution.* 59:2437–2479.

700 Barraclough, T. G., and A. P. Vogler. 2000. Detecting the geographical pattern of speciation
701 from species-level phylogenies. *Am. Nat.* 155:419–434.

- 702 Barthlott, W., J. Mutke, D. Rafiqpoor, G. Kier, and H. Kreft. 2005. Global Centers of
703 Vascular Plant Diversity. *Nov. Acta Leopoldina* NF 92:61–83.
- 704 Bhattarai, K. R., O. R. Vetaas, and J. A. Grytnes. 2004. Fern species richness along a
705 central Himalayan elevational gradient, Nepal. *J. Biogeogr.* 31:389–400.
- 706 Bouckaert, R., J. Heled, D. Kühnert, T. Vaughan, C. H. Wu, D. Xie, M. A. Suchard, A.
707 Rambaut, and A. J. Drummond. 2014. BEAST 2: A Software Platform for Bayesian
708 Evolutionary Analysis. *PLoS Comput. Biol.* 10:1–6.
- 709 Broennimann, O., M. C. Fitzpatrick, P. B. Pearman, B. Petitpierre, L. Pellissier, N. G.
710 Yoccoz, W. Thuiller, M. J. Fortin, C. Randin, N. E. Zimmermann, et al. 2012.
711 Measuring ecological niche overlap from occurrence and spatial environmental data.
712 *Glob. Ecol. Biogeogr.* 21:481–497.
- 713 Broennimann, V. D. C., and A. Guisan. 2018. *ecospat: Spatial Ecology Miscellaneous*
714 *Methods*. R package version 3.0. <https://CRAN.R-project.org/package=ecospat>
- 715 Brown, J. W., J. F. Walker, and S. A. Smith. 2017. *Phyx: Phylogenetic tools for unix*.
716 *Bioinformatics* 33:1886–1888.
- 717 Cadena, C. D., K. H. Kozak, J. L. Parra, C. M. McCain, J. P. Go, C. K. Bowie, A. C.
718 Carnaval, C. Moritz, C. Rahbek, T. E. Roberts, et al. 2012. Latitude, elevational
719 climatic zonation and speciation in New World vertebrates. *Proc. R. Soc. B Biol. Sci.*
720 279:194–201.

- 721 Capella-Gutiérrez, S., J. M. Silla-Martínez, and T. Gabaldón. 2009. trimAl: A tool for
722 automated alignment trimming in large-scale phylogenetic analyses. *Bioinformatics*
723 25:1972–1973.
- 724 Carlsen, M. M., T. Fér, R. Schmickl, J. Leong-Škorničková, M. Newman, and W. J. Kress.
725 2018. Resolving the rapid plant radiation of early diverging lineages in the tropical
726 Zingiberales: Pushing the limits of genomic data. *Mol. Phylogenet. Evol.* 128:55–68.
- 727 Chen, G. F. 2013. Sexual isolation in two bee-pollinated *Costus* (Costaceae). *Plant Reprod.*
728 26:3–16.
- 729 Chen, G. F., and D. W. Schemske. 2015. Ecological differentiation and local adaptation in
730 two sister species of Neotropical *Costus* (Costaceae). *Ecology* 96:440–449.
- 731 Contreras-Ortiz, N., G. Atchison, C. Hughes, and S. Madriñán. 2018. Convergent evolution
732 of high elevation plant growth forms and geographically structured variation in
733 Andean *Lupinus* (Leguminosae). *Bot. J. Linn. Soc.* 187:118–136.
- 734 Cortés, A. J., L. N. Garzón, J. B. Valencia, and S. Madriñán. 2018. On the causes of rapid
735 diversification in the páramos: isolation by ecology and genomic divergence in
736 *Espeletia*. *Front. Plant Sci.* 9.
- 737 De Cáceres, M., P. Legendre, R. Valencia, M. Cao, L. Chang, G. Chuyong, R. Condit, Z.
738 Hao, C-F Hsieh, S. Hubbell, et al. 2012. The variation of tree beta diversity across a
739 global network of forest plots. *Global Ecology and Biogeography* 21:1191–1202.

- 740 Diazgranados, M., and J. Barber. 2017. Geography shapes the phylogeny of frailejones
741 (Espeletiinae Cuatrec., Asteraceae): a remarkable example of recent rapid radiation in
742 sky islands. *PeerJ* 5:e2968.
- 743 Dick, C. W., and R. T. Pennington. 2019. History and geography of Neotropical tree
744 diversity. *Annu. Rev. Ecol. Evol. Syst.* 50:579–301.
- 745 Dobzhansky, T. 1950. Evolution in the Tropics. *Am. Sci.* 38:208–221.
- 746 Dormann, C. F. 2007. Effects of incorporating spatial autocorrelation into the analysis of
747 species distribution data. *Glob. Ecol. Biogeogr.* 16:129–138.
- 748 Driese, S. G., K. H. Orvis, S. P. Horn, Z. H. Li, and D. S. Jennings. 2007. Paleosol evidence
749 for Quaternary uplift and for climate and ecosystem changes in the Cordillera de
750 Talamanca, Costa Rica. *Palaeogeogr. Palaeoclimatol. Palaeoecol.* 248:1–23.
- 751 Drummond, C. S., R. J. Eastwood, S. T. S. Miotto, and C. E. Hughes. 2012. Multiple
752 continental radiations and correlates of diversification in *Lupinus* (Leguminosae):
753 testing for key innovation with incomplete taxon sampling. *Syst. Biol.* 61:443–460.
- 754 Edgar, R. C. 2010. Search and clustering orders of magnitude faster than BLAST.
755 *Bioinformatics* 26:2460–2461.
- 756 ESRI. 2018. Environmental System Research Institute (ESRI) ArcGIS release 10.6.1. ESRI,
757 Redlands, CA.

- 758 Fine, P. V. A., D. C. Daly, G. Villa, I. Mesones, K. M. Cameron, G. V. Muñoz, I. Mesones,
759 and K. M. Cameron. 2005. The contribution of edaphic heterogeneity to the evolution
760 and diversity of Burseraceae trees in the western Amazon. *Evolution* 59:1464.
- 761 Fine, P. V. A., F. Zapata, and D. C. Daly. 2014. Investigating processes of neotropical rain
762 forest tree diversification by examining the evolution and historical biogeography of
763 the Protieae (Burseraceae). *Evolution* 68:1988–2004.
- 764 Fitzpatrick, B. M., and M. Turelli. 2006. The geography of mammalian speciation: mixed
765 signals from phylogenies and range maps. *Evolution* 60:601–615.
- 766 Friis, E. 1988. *Spirematospermum chandlerae* sp. nov., an extinct species of Zingiberaceae
767 from the North American Cretaceous. *Tertiary Res.* 9:7–12.
- 768 Fox, J., and S. Weisberg. 2019. *An R Companion to Applied Regression, Third Edition.*
769 Sage, Thousand Oaks, CA.
- 770 Gaboriau, T., F. Leprieur, D. Mouillot, and N. Hubert. 2018. Influence of the Geography of
771 Speciation on Current Patterns of Coral Reef Fish Biodiversity across the Indo-Pacific.
772 *Ecography* 41(8): 1295–1306.
- 773 Gentry, A. H. 1982. Neotropical Floristic Diversity□: Phytogeographical Connections
774 Between Central and South America , Pleistocene Climatic Fluctuations , or an
775 Accident of the Andean Orogeny? *Ann. Missouri Bot. Gard.* 69:557–593.

- 776 Ghalambor, C. K., R. B. Huey, P. R. Martin, J. Tweksbury, and G. Wang. 2006. Are
777 mountain passes higher in the tropics? Janzen's hypothesis revisited. *Integr. Comp.*
778 *Biol.* 46:5–17.
- 779 Gotelli, N.J. and R.K. Colwell. 2001. Quantifying biodiversity: procedures and pitfalls in
780 the measurement and comparison of species richness. *Ecol. Lett.* 4:379-391.
- 781 Grabherr, M. G., B. J. Haas, M. Yassour, J. Z. Levin, D. A. Thompson, I. Amit, X.
782 Adiconis, L. Fan, R. Raychowdhury, Q. Zeng, et al. 2011. Full-length transcriptome
783 assembly from RNA-Seq data without a reference genome. *Nat. Biotechnol.* 29:644–
784 652.
- 785 Gregory-Wodzicki, K. M. 2000. Uplift history of the Central and Northern Andes: a review.
786 *Geol. Soc. Am. Bull.* 112:1091–1105.
- 787 Grossenbacher, D. L., S. D. Veloz, and J. P. Sexton. 2014. Niche and range size patterns
788 suggest that speciation begins in small, ecologically diverged populations in north
789 american monkeyflowers (*Mimulus* spp.). *Evolution* 68:1270–1280.
- 790 Grytnes, J.A. and J.H. Beaman. 2006. Elevational species richness patterns for vascular
791 plants on Mount Kinabalu, Borneo. *J. Biogeogr.* 33:1838–1849.
- 792 Guarnizo, C. E., and D. C. Cannatella. 2013. Genetic divergence within frog species is
793 greater in topographically more complex regions. *J. Zool. Syst. Evol. Res.* 51:333–340.

- 794 Guisan, A., and C. Rahbek. 2011. SESAM - a new framework integrating macroecological
795 and species distribution models for predicting spatio-temporal patterns of species
796 assemblages. *J. Biogeogr.* 38:1433–1444.
- 797 Hickey, L.J., Peterson, R.K., 1978. *Zingiberopsis*, a fossil genus of the ginger family from
798 Late Cretaceous to early Eocene sediments of western interior North America. *Can. J.*
799 *Bot.* 56, 1136–1152.
- 800 Hijmans, R. J. 2019. Raster: geographic data and modelling. R package version 2.9-5.
801 <https://CRAN.R-project.org/package=raster>
- 802 Hughes, C. E., and G. W. Atchison. 2015. The ubiquity of alpine plant radiations□: from
803 the Andes to the Hengduan Mountains. *New Phytol.* 207:275–282.
- 804 Janzen, D. H. 1967. Why mountain passes are higher in the tropics. *Am. Nat.* 101:233–249.
- 805 Johnson, M. G., E. M. Gardner, Y. Liu, R. Medina, B. Goffinet, A. J. Shaw, N. J. C. Zerega,
806 and N. J. Wickett. 2016. HybPiper: Extracting Coding Sequence and Introns for
807 Phylogenetics from High-Throughput Sequencing Reads Using Target Enrichment.
808 *Appl. Plant Sci.* 4:1600016.
- 809 Katoh, K., and D. M. Standley. 2013. MAFFT multiple sequence alignment software
810 version 7: Improvements in performance and usability. *Mol. Biol. Evol.* 30:772–780.
- 811 Kay, K. M. 2006. Reproductive isolation between two closely related hummingbird-
812 pollinated Neotropical gingers. *Evolution* 60:538.

- 813 Kay, K. M., and D. W. Schemske. 2003. Pollinator assemblages and visitation rates for 11
814 species of Neotropical *Costus* (Costaceae). *Biotropica* 35:198.
- 815 Kay, K. M., and D. W. Schemske. 2008. Natural selection reinforces speciation in a
816 radiation of neotropical rainforest plants. *Evolution* 62:2628–2642.
- 817 Kay, K. M., P. A. Reeves, R. G. Olmstead, and D. W. Schemske. 2005. Rapid speciation
818 and the evolution of hummingbird pollination in neotropical *Costus* subgenus *Costus*
819 (Costaceae): Evidence from nrDNA its and ETS sequences. *Am. J. Bot.* 92:1899–1910.
- 820 Kissling, W.D., and G. Carl. 2008. Spatial autocorrelation and the selection of simultaneous
821 autoregressive models. *Glob. Ecol. Biogeogr.* 17:59–71.
- 822 Lagomarsino, L. P., F. L. Condamine, A. Antonelli, A. Mulch, and C. C. Davis. 2016. The
823 abiotic and biotic drivers of rapid diversification in Andean bellflowers
824 (Campanulaceae). *New Phytol.* 210:1430–1442.
- 825 Landis, M. J., N. J. Matzke, B. R. Moore, and J. P. Huelsenbeck. 2013. Bayesian analysis of
826 biogeography when the number of areas is large. *Syst. Biol.* 62:789–804.
- 827 Luebert, F., and M. Weigend. 2014. Phylogenetic insights into Andean plant diversification.
828 *Front. Ecol. Evol.* 2:1–17.
- 829 Maas, P. J. M. 1972. Costoideae (Zingiberaceae). *Flora Neotrop.* 8:1–139.
- 830 Maas, P. J. M. 1977. *Renealmia* (Zingiberaceae - Zingiberoideae) Costoideae (additions)
831 (Zingiberaceae). *Flora Neotrop.* 18:1–218.

- 832 Maddison, W.P. and R.G. FitzJohn. 2015. The unsolved challenge to phylogenetic
833 correlation tests for categorical characters. *Syst. Biol.* 64:127-136.
- 834 Madriñán, S., A. J. Cortés, and J. E. Richardson. 2013. Páramo is the world's fastest
835 evolving and coolest biodiversity hotspot. *Front. Genet.* 4:192.
- 836 Mai, U., and S. Mirarab. 2018. TreeShrink: Fast and accurate detection of outlier long
837 branches in collections of phylogenetic trees. *BMC Genomics* 19:272.
- 838 Matzke, N. J. 2013. BioGeoBEARS: Biogeography with Bayesian (and likelihood)
839 evolutionary analysis in R Scripts, CRAN: The Comprehensive R Archive Network,
840 Vienna, Austria.
- 841 Mayr, E. 1954. Change of genetic environment and evolution. Pp. 157–180 in J. Huxley, A.
842 C. Hardy, and E. B. Ford, eds. *Evolution as a process*. Collier Books, New York.
- 843 Mayr, E. 1982. Processes of speciation in animals. Pp. 1–19 in C. Barigozzi, ed.
844 *Mechanisms of speciation*. Alan R. Liss, New York.
- 845 Misiewicz, T. M., and P. V. A. Fine. 2014. Evidence for ecological divergence across a
846 mosaic of soil types in an Amazonian tropical tree: *Protium subserratum*
847 (Burseraceae). *Mol. Ecol.* 23:2543–2558.
- 848 Morales-Briones, D. F., K. Romoleroux, F. Kolář, and D. C. Tank. 2018. Phylogeny and
849 evolution of the neotropical radiation of *Lachemilla* (Rosaceae): uncovering a history
850 of reticulate evolution and implications for infrageneric classification. *Syst. Bot.*
851 43:17–34.

- 852 Morrone, J. J. 2014. Biogeographical regionalisation of the neotropical region. *Zootaxa*
853 3782:1–110.
- 854 Nevado, B., G. W. Atchison, C. E. Hughes, and D. A. Filatov. 2016. Widespread adaptive
855 evolution during repeated evolutionary radiations in New World lupins. *Nat. Commun.*
856 7:12384.
- 857 Nguyen, L. T., H. A. Schmidt, A. Von Haeseler, and B. Q. Minh. 2015. IQ-TREE: A fast
858 and effective stochastic algorithm for estimating maximum-likelihood phylogenies.
859 *Mol. Biol. Evol.* 32:268–274.
- 860 Pagel M. 1994. Detecting correlated evolution on phylogenies: a general method for the
861 comparative analysis of discrete characters. *Proceedings: Biological Sciences* 255: 37–
862 45.
- 863 Palma-Silva, C., T. Wendt, F. Pinheiro, T. Barbará, M. F. Fay, S. Cozzolino, and C. Lexer.
864 2011. Sympatric bromeliad species (*Pitcairnia* spp.) facilitate tests of mechanisms
865 involved in species cohesion and reproductive isolation in Neotropical inselbergs. *Mol.*
866 *Ecol.* 20:3185–3201.
- 867 Pasek, J. 2020. Weights: Weighting and Weighted Statistics. R package version 1.0.1.
868 <https://CRAN.R-project.org/package=weights>
- 869 Pomara, L. Y., K. Ruokolainen, H. Tuomisto, and K. R. Young. 2012. Avian composition
870 co-varies with floristic composition and soil nutrient concentration in Amazonian
871 upland forests. *Biotropica* 44: 545–53.

- 872 Pyron, R. A., G. C. Costa, M. A. Patten, and F. T. Burbrink. 2015. Phylogenetic niche
873 conservatism and the evolutionary basis of ecological speciation. *Biol. Rev.* 90:1248–
874 1262.
- 875 R Core Team. 2020. R: A Language and Environment for Statistical Computing. Vienna,
876 Austria.
- 877 Rahbek, C., M. K. Borregaard, A. Antonelli, R. K. Colwell, B. G. Holt, D. Nogues-Bravo,
878 C. M. Ø. Rasmussen, K. Richardson, M. T. Rosing, R. J. Whittaker, and J. Fjeldså.
879 2019a. Building mountain biodiversity: Geological and evolutionary processes.
880 *Science* 365:1114–1119.
- 881 Rahbek, C., M. K. Borregaard, R. K. Colwell, B. Dalsgaard, B. G. Holt, N. Morueta-Holme,
882 D. Nogues-Bravo, R. J. Whittaker, and J. Fjeldså. 2019. Humboldt’s enigma: What
883 causes global patterns of mountain biodiversity? *Science* 365:1108–1113.
- 884 Rambaut, A., M. A. Suchard, D. Xie, and A. J. Drummond. 2014. Tracer v1.6.
885 <http://beast.bio.ed.ac.uk/Tracer>
- 886 Ree, R. H., and I. Sanmartín. 2018. Conceptual and statistical problems with the DEC+J
887 model of founder-event speciation and its comparison with DEC via model selection. *J.*
888 *Biogeogr.* 45:741–749.
- 889 Ree, R. H., and S. A. Smith. 2008. Maximum Likelihood Inference of Geographic Range
890 Evolution by Dispersal, Local Extinction, and Cladogenesis. *Syst. Biol.* 57:4–14.

- 891 Revell, L. J. 2012. phytools: An R package for phylogenetic comparative biology (and other
892 things). *Methods Ecol. Evol.* 3:217–223.
- 893 Riley, S. J., S. D. DeGloria, and R. Elliot. 1999. A terrain ruggedness index that quantifies
894 topographic heterogeneity. *Intermountain Journal of Sciences* 5:1–4.
- 895 Roalson, E. H., and W. R. Roberts. 2016. Distinct processes drive diversification in
896 different clades of Gesneriaceae. *Syst. Biol.* 65:662–684.
- 897 Ronquist, F. 1997. Dispersal-Vicariance Analysis: A new approach to the quantification of
898 historical biogeography. *Syst. Biol.* 46:195–203.
- 899 Salzman, S., H. E. Driscoll, T. Renner, T. André, S. Shen, and C. D. Specht. 2015. Spiraling
900 into history: a molecular phylogeny and investigation of biogeographic origins and
901 floral evolution for the genus *Costus*. *Syst. Bot.* 40:104–115.
- 902 Sheldon, K. S., R. B. Huey, M. Kaspari, and N. J. Sanders. 2018. Fifty years of mountain
903 passes: a perspective on Dan Janzen’s classic article. *Am. Nat.* 191:553–565.
- 904 Smith, S. A., and B. C. O’Meara. 2012. TreePL: Divergence time estimation using
905 penalized likelihood for large phylogenies. *Bioinformatics* 28:2689–2690.
- 906 Smith, S. A., M. J. Moore, J. W. Brown, and Y. Yang. 2015. Analysis of phylogenomic
907 datasets reveals conflict, concordance, and gene duplications with examples from
908 animals and plants. *BMC Evol. Biol.* 15:150.
- 909 Smith, S. A., J. W. Brown, and J. F. Walker. 2018. So many genes, so little time: A
910 practical approach to divergence-time estimation in the genomic era. *PLoS One* 13.

- 911 Stiles, G. F. 1981. Geographical aspects of bird-flower coevolution, with particular
912 reference to Central America. *Ann. Missouri Bot. Gard.* 68:323–351.
- 913 ter Steege, H and Amazon Tree Diversity Network. 2010. RAINFOR (Amazon Forest
914 Inventory Network). Pp. 349–359 *in* C. Hoorn and F. Wesselingh eds. *Amazonia:*
915 *Landscape and Species Evolution.* Wiley, Oxford, UK.
- 916 Tripp, E. A., and Y. H. E. Tsai. 2017. Disentangling geographical, biotic, and abiotic
917 drivers of plant diversity in neotropical *Ruellia* (Acanthaceae). *PLoS One* 12:1–17.
- 918 Uribe-Convers, S., and D. C. Tank. 2015. Shifts in diversification rates linked to
919 biogeographic movement into new areas: An example of a recent radiation in the
920 andes. *Am. J. Bot.* 102:1854–1869.
- 921 Vargas, O. M., E. M. Ortiz, and B. B. Simpson. 2017. Conflicting phylogenomic signals
922 reveal a pattern of reticulate evolution in a recent high-Andean diversification
923 (Asteraceae: Astereae: *Diplostephium*). *New Phytol.* 214:1736–1750.
- 924 Vargas, O. M., M. Heuertz, S. A. Smith, and C. W. Dick. 2019. Target sequence capture in
925 the Brazil nut family (Lecythidaceae): Marker selection and in silico capture from
926 genome skimming data. *Mol. Phylogenet. Evol.* 135:98–104.
- 927 Vargas, O. M., and C. W. Dick. 2020. Diversification history of neotropical Lecythidaceae,
928 an ecologically dominant tree family of Amazon Rain Forest. Pp. 791–809 *in* V. Rull
929 and A. C. Carnaval, eds. *Neotropical Diversification.* Springer, Cham, Switzerland.

- 930 Vargas, O. M., and B. B. Simpson. 2019. Allopatric speciation is more prevalent than
931 parapatric ecological divergence in tropical montane systems (Asteraceae: *Piofontia*).
932 BioRxiv 1–32. <https://doi.org/10.1101/868216>
- 933 Warren, D. L., R. E. Glor, and M. Turelli. 2008. Environmental niche equivalency versus
934 conservatism: Quantitative approaches to niche evolution. *Evolution* 62:2868–2883.
- 935 Weir, J. T., and D. Schuller. 2008. The latitudinal gradient in recent speciation and
936 extinction rates of birds and mammals. *Science* 315:1574–1577.
- 937 Yu, G., D. K. Smith, H. Zhu, Y. Guan, and T. T. Y. Lam. 2017. Ggtree: an R package for
938 visualization and annotation of phylogenetic trees with their covariates and other
939 associated data. *Methods Ecol. Evol.* 8:28–36.
- 940 Zhang, C., E. Sayyari, and S. Mirarab. 2017. ASTRAL-III: increased scalability and
941 impacts of contracting low support branches. Pp. 53–75 *in* J. Meidanis and L. Nakhleh,
942 eds. *Comparative Genomics*. Springer, Cham, Switzerland.
- 943 Zhbannikov, I. Y., S. S. Hunter, J. A. Foster, and M. L. Settles. 2017. SeqyClean: A
944 Pipeline for High-throughput Sequence Data Preprocessing. Pp. 407–416 *in*
945 *Proceedings of the 8th ACM International Conference on Bioinformatics,*
946 *Computational Biology, and Health Informatics*. ACM, New York, NY, USA.